Design and Demonstration of Ultra-thin 3D Glass-based 5G Modules with Low-loss Interconnects

Atom O. Watanabe[1], Tong-Hong Lin[1], Tomonori Ogawa[2], P. Markondeya Raj[1], Venkatesh Sundaram[1], Manos M. Tentzeris[1], and Rao R. Tummala[1]
[1]*3D System Packaging Research Center, Georgia Institute of Technology, Atlanta, GA 30332, USA*
[2]*Asahi Glass Company, Tokyo, Japan*

***Abstract*— This paper demonstrates six-metal-layer antenna-to-receiver signal transitions on panel-scale processed ultra-thin glass-based 5G module substrates with 50-Ω transmission lines and micro-via transitions in re-distribution layers. The glass modules consist of low-loss dielectric thin-films laminated on 100-μm glass cores. Modeling, design, fabrication, and characterization of the multilayered signal interconnects were performed at 28-GHz band. The surface planarity and dimensional stability of glass substrates enabled the fabrication of highly-controlled signal traces with tolerances of 2% inside the re-distribution layers on low-loss dielectric build-up thin-films. The fabricated transmission lines showed 0.435 dB loss with 4.19 mm length, while microvias in low-loss dielectric thin-films showed 0.034 dB/microvia. The superiority of glass substrates enable low-loss link budget with high precision from chip to antenna for 5G communications.**

Keywords*— 5G, Glass substrates, Low loss interconnects, re-distribution layer.

I. Introduction

Fifth-generation (5G) communication technology has been gaining more attention for various applications such as Internet of Things (IoTs), high-definition video streaming, fast large-file transfer, and vehicle-to-everything (V2X) communications [1]. The main benefits of 5G technology includes 10X-100X higher data rate, massive device connectivity, lower end-to-end latency, and consistent quality of experience provisioning [2]. In addition to millimeter-wave radio solutions developed for radar and Lidar applications [3], significant progress of such high-frequency systems has been made in standards, regulations, and solutions for consumer daily use. Various mm-wave bands ranging from 10 GHz through 100 GHz are currently expected to be used in 5G mobile communication systems to enable wide transmission bandwidth. Especially, industry and academia are mainly focusing on frequency bands around 28, 38–39, 60, and 73 GHz [4], [5].

These 5G communication systems are, however, facing various types of technical challenges, one of which is the constraints of link budget because of the large propagation loss and low transmit power that are characteristic to mm-wavelength electromagnetic (EM) waves. Therefore, control of the link budget from chip to antenna is getting more important to achieve ultra-high data-rate communications. For low signal losses, high performance of antennas, and system integration, a wide variety of substrate technologies have been explored [4]. In general, ultra-low loss organics based on Teflon and liquid-crystal polymers (LCP) [6], low-temperature co-fired ceramic substrates (LTCC) [7], silicon substrates, and molding-compound-based fan-out wafer-level packages (FOWLP) [8], [9] are explored and developed for the 5G packaging technology. From the architecture standpoint, a fully-integrated antenna-in-package (AiP) solution [5] is emerging as the key solution to meet multiple requirements such as low noise figure from antenna to chip, low-loss link budget, frequency-band control, antenna array performance, form factor, and reliability.

However, state-of-the-art mm-wave packaging technologies are not able to handle high precision and tolerance of high-density mm-wave components that have been continuously scaling down the features in emerging communication systems. They also confront form-factor challenges because of the multiple layers needed for signal re-distributions. In order to address these challenges, glass-based packages have been gaining attention for 5G applications [10], [11], [12] because of superior dimensional stability [13], tolerance to external environment, ability to form fine-pitch line and spaces [14] and through vias [15], coefficient of thermal expansion (CTE) match with dies, low-loss dielectric properties compared to silicon or molding-compound-based substrates, and availability in large-area cost-effective panels [16].

In order to demonstrate the benefits of glass-based packages for 5G applications, this paper focuses on achieving low-loss link budget from chip to antenna and precision in fabrication of transmission lines and microvias on re-distribution layers (RDL) with low-loss dielectric buildup materials that are fabricated on 100-μm glass substrates.

II. Modeling and Design of Six-Metal-Layer Test Vehicles with Transmission Lines and Microvias

The objective of this task is to demonstrate superior performance of RDL on thin glass substrates (100 μm) with low-loss dielectric thin-films, using six-metal-layer test vehicles shown in Figure 1. EN-A1 from Asahi Glass is selected as the glass core substrate, and GL102 from Ajinomoto is chosen as the dielectric because of its superior handling and low dielectric constant and low loss tangent.The test vehicles include transmission lines such as microstrip lines with a width of 66 μm (Figure 2 (a)), striplines with a width of 6.6 μm (Figure 2 (b)), and the combination of the transmission lines with microvias (Figure 2 (c)) so that the interconnects have 50 Ω characteristic impedance at 28 GHz. The microvias were designed to have a diameter of 40 μm for seamless transitions from microstrip lines on M1/M6 to striplines on M2/M5, while M3 and M4 metal layers act as reference or ground planes.

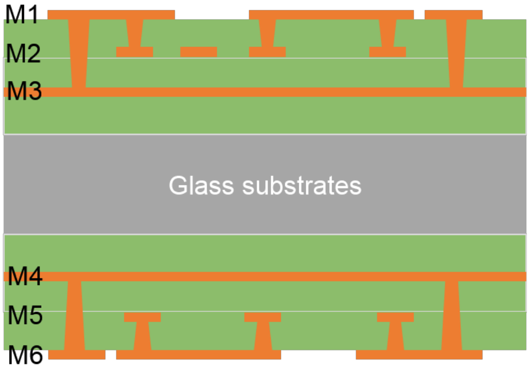

Fig. 1. Cross-section image of the designed six-metal-layer test vehicles

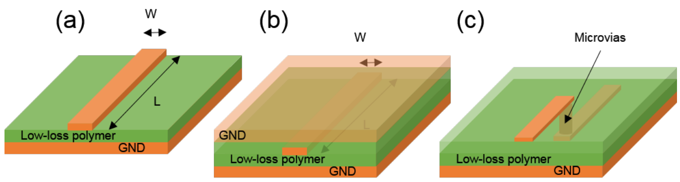

Fig. 2. Interconnect structures with (a) microstrip lines, (b) striplines, and (c) microvias.

In order to obtain the losses from transmission lines and microvias separately, interconnect structures with and without microvia-transitions were designed. The frequency responses simulated in a 3D full-wave EM simulator indicate that the insertion losses, S_{21}, of the transmission lines on RDL are as low as 0.066 dB/mm. Ultra-short microvias of 7-μm enabled low insertion loss of 0.032 dB/microvia. These results are illustrated in Figure 3.

III. PRECISION OF FABRICATED SIX-METAL-LAYER RDL ON LAMINATED GLASS

In order to validate the designs, fabrication of the six metal layers on two glass panels was performed using the semi-additive patterning (SAP) process, as shown in Figure 4. Figure 4 (b) and (c) illustrate the 50 Ω impedance-matched microstrip lines and the combination of microstrip lines, striplines, and microvias, respectively. Inspection was performed through 3D optical microscopy to investigate the fabrication precision of RDL, and the results are summarized in Table I. In the test vehicles, the microstrip lines were designed with two types of widths, considering over-etching during the electroless seed layer etching; one is the target width (i.e., 65.6 μm) and the other is 2 μm wider than the target width (i.e., 67.6 μm). The widths obtained

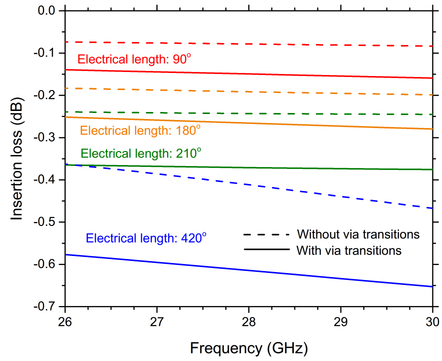

Fig. 3. Interconnect structures with (a) microstrip lines, (b) striplines, and (c) microvias.

through the inspections are the averaged numbers of more than thirty coupons in each test vehicle. It is found that the SAP technique on glass substrates designed for 5G applications provides high precision control with variances less than 2%. Miniaturized interconnects or passive structures integrated in RDL requires fine features with high precision in mm-wave frequencies especially in order to obtain the designed impedance for such structures and, thus, the desired frequency responses. The precision of narrow transmission lines (< 10 μm) is expected to be higher with glass substrates because of enhanced smoothness and less warpage with many RDL, when compared to organic core substrates.

In addition to the in-plane inspections discussed above, cross sectioning of the six-metal-layer stackups was performed as shown in Figure 5. Although copper thickness of 7.4 μm in M2 is close to the target thickness of 7.5 μm, the thickness of 5.8 μm in M1 is slightly lower than the target, which might increase the impedance of microstrip lines depicted in the right part of Figure 5. In addition, low-loss dielectric buildup layers below M2 and M3 showed thickness of 13.2–13.6 μm, while the target was 15 μm; similarly, the thickness of the dielectric between M1 and M2 was 9.0 μm, where the one simulated in the modeled was 8.0 μm. These differences might cause discrepancy in characteristic impedance modeled in Section II, which leads to impedance mismatching or higher signal transmission loss. Characterization of electrical performance of the fabricated test vehicles is discussed in Section IV

TABLE I
RDL PRECISION FABRICATED IN LOW-LOSS POLYMER LAMINATED ON GLASS SUBSTRATES

	Glass TV#1		Glass TV#2	
	Transmission lines			
Target	65.6	67.6	65.6	67.6
Measurements	65.13	65.09	67.11	67.15
Variance	0.95	0.64	1.34	0.53
Precision	1.46%	0.98%	1.99%	0.79%

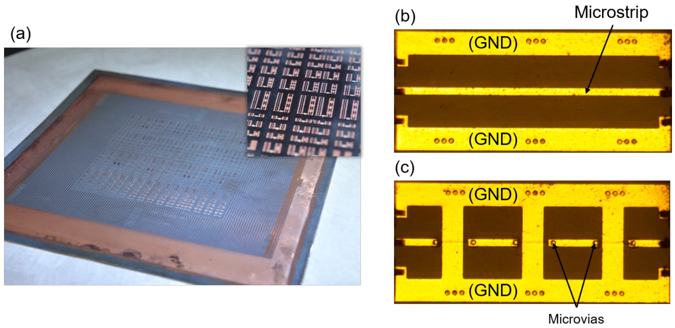

Fig. 4. Fabricated test vehicles (a) laminated-glass panel (b) top view of microstrip lines without transitions (c) top view of microstrip and striplines with microvia transitions.

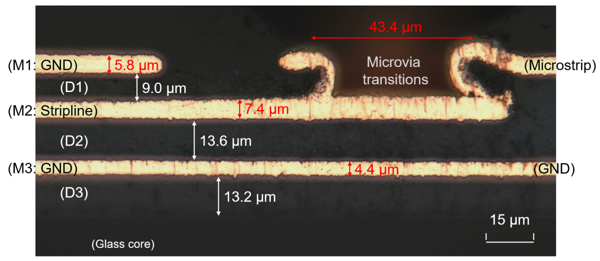

Fig. 5. Cross-section image of the top three metal layers with low-loss dielectric film laminated on glass core substrates.

IV. ELECTRICAL CHARACTERIZATION AND ANALYSES OF SIX-METAL-LAYER INTERCONNECTS

Utilizing the fabricated six-metal-layer test vehicles on glass substrates, high-frequency measurements of transmission lines with and without transitions were performed through a vector network analyzer (VNA) that is calibrated up to 40 GHz. The insertion losses through HFSS simulations and measurements through VNA are compared to quantify the transmission-line and microvia losses and the deviation in the impedance matching due to the fabrication discussed in Section III. Figure 6 shows insertion losses of (a) microstrip lines and (b) the combination of microstrip lines and striplines connected with microvias, as a function of frequency in the vicinity of 28 GHz The measurement results indicate reasonable consistency with simulation results. The insertion losses in transmission lines and microvias are summarized in Tables II and III, respectively. Insertion losses of more than twenty coupons are averaged to remove bias caused by selection of locations to be measured.

Measurement results calculated by linear regression show an averaged insertion loss of 0.105 dB/mm with 15 μm low-loss dielectric thin-films, which is 6% higher than that obrained from the simulation results. The higher losses are attributed to several factors; one of the primary factors is the copper roughness that was not taken into account in HFSS simulations. Another key factor is the variation of thickness of dielectric films and copper traces; as discussed in Section III, the thickness of dielectric and copper traces were slightly different from the designed ones. This causes

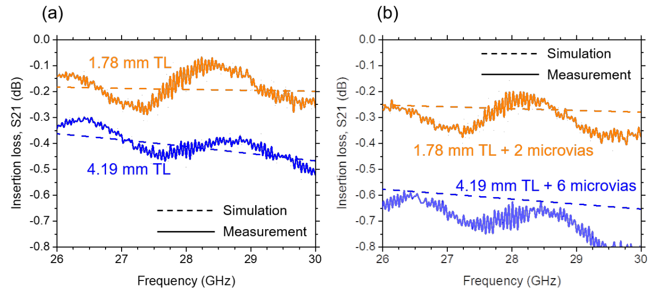

Fig. 6. Insertion loss of transmission line structures (a) without and (b) with microvia transitions.

TABLE II
INSERTION LOSS OF THE COMBINATION OF MICROSTRIP LINES AND STRIPLINES

Transmission line length (mm)	Transmission line losses (dB)	
	Simulation	Measurement
0.95	-0.079	-0.088
1.78	-0.192	-0.218
2.29	-0.243	-0.235
4.19	-0.412	-0.435
Insertion loss per unit length (dB/mm)	-0.099	-0.105

changes in the impedance of transmission lines. Therefore, frequency responses in Figure 6 show ripples that do not appear if systems are perfectly matched with 50 Ω. Although the variation of transmission-line widths listed in Table I lead to certain impedance mismatch, high precision (< 2%) fabrication with glass will not significantly change the impedance of the transmission lines.

Similarly, measurement results in Table III show insertion loss of 0.034 dB/microvia, which is 6% higher than that obtained from simulations. This discrepancy is mainly caused by the difference in microvia topologies assumed in the modeling and that fabricated in the actual test vehicles; while conformal vias are fabricated as shown in Figure 5, fully-filled microvias are assumed in the 3D full-wave EM solvers to reduce the simulation complexity. Conformal vias yield higher resistance and parasitic inductance compared to fully-filled vias, causing impedance mismatch and thus higher loss, as observed in Table III.

TABLE III
INSERTION LOSS OF MICROVIAS

Number of microvias	Microvia losses	
	Simulation	Measurement
2	-0.073	-0.062
6	-0.165	-0.216
Insertion loss per microvia (dB/microvia)	-0.032	-0.034

V. CONCLUSIONS

This paper demonstrated six-metal-layer antenna-to-receiver signal transitions on panel-scale processed ultra-thin glass-based 5G modules with 50-Ω transmission lines and micro-via transitions in re-distribution layers consisting of copper traces or planes and low-loss dielectric thin-films laminated on 100-μm glass substrates. In order to show the benefits of glass for 5G communications, modeling, design, fabrication, and characterization of the signal interconnects were performed at the 28 GHz band. Excellent surface planarity and dimensional stability of glass substrates resulted in high-precision transmission lines with tolerances within 2%. Microvias in RDL were also fabricated with high precision ($< 2\%$). The measurement results of the fabricated signal traces and microvias in low-loss dielectric showed insertion loss of 0.099 dB/mm and 0.032 dB/microvia, respectively. The low-loss link budget from chip to package-integrated-antennas, thus, makes glass a compelling substrate candidate for emerging 5G communication systems.

ACKNOWLEDGMENT

The authors wish to acknowledge Hiroyuki Matsuura for helping with the fabrication of test vehicles. They also would like to thank the industry sponsors of the consortia program at Georgia-Tech Packaging Research Center (GT-PRC) for their technical guidance and support.

REFERENCES

[1] I. F. Akyildiz, S. Nie, S.-C. Lin, and M. Chandrasekaran, "5g roadmap: 10 key enabling technologies," *Computer Networks*, vol. 106, pp. 17–48, 2016.

[2] W. Hong, K. Baek, Y. Lee, and Y. G. Kim, "Design and analysis of a low-profile 28 ghz beam steering antenna solution for future 5g cellular applications," in *Microwave Symposium (IMS), 2014 IEEE MTT-S International*. IEEE, 2014, pp. 1–4.

[3] T. Kamgaing, A. A. Elsherbini, T. W. Frank, S. N. Oster, and V. R. Rao, "Investigation of a photodefinable glass substrate for millimeter-wave radios on package," in *Electronic Components and Technology Conference (ECTC), 2014 IEEE 64th*. IEEE, 2014, pp. 1610–1615.

[4] D. Liu, X. Gu, C. W. Baks, and A. Valdes-Garcia, "Antenna-in-package design considerations for ka-band 5g communication applications," *IEEE Transactions on Antennas and Propagation*, vol. 65, no. 12, pp. 6372–6379, 2017.

[5] D. Liu and Y. Zhang, "Integration of array antennas in chip package for 60-ghz radios," *Proceedings of the IEEE*, vol. 100, no. 7, pp. 2364–2371, 2012.

[6] C.-Y. Ho, M.-F. Jhong, P.-C. Pan, C.-Y. Huang, C.-C. Wang, and C.-Y. Ting, "Integrated antenna-in-package on low-cost organic substrate for millimeter-wave wireless communication applications," in *Electronic Components and Technology Conference (ECTC), 2017 IEEE 67th*. IEEE, 2017, pp. 242–247.

[7] Y. P. Zhang and D. Liu, "Antenna-on-chip and antenna-in-package solutions to highly integrated millimeter-wave devices for wireless communications," *IEEE Transactions on Antennas and Propagation*, vol. 57, no. 10, pp. 2830–2841, 2009.

[8] C.-H. Tsai, J.-S. Hsieh, M. Liu, E.-H. Yeh, H.-H. Chen, C.-W. Hsiao, C.-S. Chen, C.-S. Liu, M.-J. Lii, C.-T. Wang *et al.*, "Array antenna integrated fan-out wafer level packaging (info-wlp) for millimeter wave system applications," in *Electron Devices Meeting (IEDM), 2013 IEEE International*. IEEE, 2013, pp. 25–1.

[9] C.-W. Hsu, C.-H. Tsai, J.-S. Hsieh, K.-C. Yee, C.-T. Wang, and D. Yu, "High performance chip-partitioned millimeter wave passive devices on smooth and fine pitch info rdl," in *Electronic Components and Technology Conference (ECTC), 2017 IEEE 67th*. IEEE, 2017, pp. 254–259.

[10] V. Sundaram, B. Deprospo, N. Gezgin, A. Watanabe, P. M. Raj, F. Liu, W. Puckett, S. Graham, R. Tummala, K. Byers *et al.*, "Integrated copper heat slugs and emi shields in panel laminate (lfo) and glass fanout (gfo) packages for high power rf ics," in *Electronic Components and Technology Conference (ECTC), 2017 IEEE 67th*. IEEE, 2017, pp. 300–305.

[11] A. O. Watanabe, M. Ali, B. Tehrani, J. Hester, H. Matsuura, T. Ogawa, P. M. Raj, V. Sundaram, M. M. Tentzeris, and R. R. Tummala, "First demonstration of 28 ghz and 39 ghz transmission lines and antennas on glass substrates for 5g modules," in *Electronic Components and Technology Conference (ECTC), 2017 IEEE 67th*. IEEE, 2017, pp. 236–241.

[12] T. H. Lin, P. M. Raj, A. Watanabe, V. Sundaram, R. Tummala, and M. M. Tentzeris, "Nanostructured miniaturized artificial magnetic conductors (amc) for high-performance antennas in 5g, iot, and smart skin applications," in *2017 IEEE 17th International Conference on Nanotechnology (IEEE-NANO)*, July 2017, pp. 911–915.

[13] S. McCann, V. Smet, V. Sundaram, R. R. Tummala, and S. K. Sitaraman, "Experimental and theoretical assessment of thin glass substrate for low warpage," *IEEE Transactions on Components, Packaging and Manufacturing Technology*, vol. 7, no. 2, pp. 178–185, 2017.

[14] F. Liu, C. Nair, A. Kubo, T. Ando, H. Lu, R. Zhang, H. Chen, K. S. Lee, V. Sundaram, and R. R. Tummala, "Via-in-trench: A revolutionary panel-based package rdl configuration capable of 200-450 io/mm/layer, an innovation for more-than-moore system integration," in *Electronic Components and Technology Conference (ECTC), 2017 IEEE 67th*. IEEE, 2017, pp. 2097–2103.

[15] S. Viswanathan, T. Ogawa, K. Demir, T. B. Huang, P. M. Raj, F. Liu, V. Sundaram, and R. Tummala, "High frequency electrical performance and thermo-mechanical reliability of fine-pitch, copper-metallized through-package-vias (tpvs) in ultra-thin glass interposers," in *Electronic Components and Technology Conference (ECTC), 2017 IEEE 67th*. IEEE, 2017, pp. 1510–1516.

[16] C. Buch, D. Struk, K. J. Wolter, P. J. Hesketh, V. Sundaram, R. Tummala, C. Shearer, J. Haley, M. Findlay, and M. Papageorge, "Design and demonstration of highly miniaturized, low cost panel level glass package for mems sensors," in *2017 IEEE 67th Electronic Components and Technology Conference (ECTC)*, May 2017, pp. 1088–1097.